Chinese Journal of Physics 68 (2020) 699–711

Contents lists available at ScienceDirect

Chinese Journal of Physics

journal homepage: www.sciencedirect.com/journal/chinese-journal-of-physics

Interaction phenomena among lump, periodic and kink wave solutions to a (3 + 1)-dimensional Sharma-Tasso-Olver-like equation

Mohammad Safi Ullah [a,b], Harun-Or Roshid [c,*], Wen-Xiu Ma [d,e,f,g], M. Zulfikar Ali [b], Zillur Rahman [a,b]

[a] Department of Mathematics, Comilla University, Cumilla-3506, Bangladesh
[b] Department of Mathematics, Rajshahi University, Rajshahi-6205, Bangladesh
[c] Department of Mathematics, Pabna University of Science and Technology, Pabna-6600, Bangladesh
[d] Department of Mathematics and Statistics, University of South Florida, Tampa, FL 33620, USA
[e] Department of Mathematics, Zhejiang Normal University, Jinhua 321004, Zhejiang, China
[f] College of Mathematics and Systems Science, Shandong University of Science and Technology, Qingdao 266590, Shandong, China
[g] Department of Mathematical Sciences, North-West University, Mafikeng Campus, Mmabatho 2735, South Africa

ARTICLE INFO

Keywords:
Sharma–Tasso–Olver-like (STOL) equation
Soliton
Lump wave
rogue wave
kinky periodic wave

PACS Nos:
02.30.Jr
02.70.Wz
05.45.Yv
94.05.Fg

ABSTRACT

In this article, we consider a (3 + 1)-dimensional Sharma–Tasso–Olver-like (STOL) model describing dynamical propagation of nonlinear dispersive waves in inhomogeneous media. Applying Hirota's bilinear technique and a trial function, we explore nonlinear dynamical properties of basic solutions to the STOL model. We find that the fission fusion pattern occurs in the collision between the lump and kink waves, the collision between the lump and periodic waves, and the collision among the lump, kink and periodic waves, which is a novel fascinating collision pattern. We also observe that a large value of the coefficient in the periodic function produces a hybrid lump wave by fission in the collision solution. To better understand the dynamic properties of the obtained collision solutions, we plot a number of 3D and contour diagrams by choosing suitable parametric values with the aid of the computational software Maple 18.

1. Introduction

Nonlinear evolution equations (NLEEs) applicable not only the areas of mathematical physics, but also other branches of nonlinear science for instance optics, plasma physics, atmospheric, geochemistry and oceanic sciences etc. [1-4]. Complication of NLEES and challenges in their analytical study has engrossed a lots of effort from renowned scientists who are involved with nonlinear dynamics. As a result, exploration of exact solutions of NLEEs is a vital anxiety for dynamical researchers. There are diverse categories of exact solutions mainly soliton, multi-soliton, rational, periodic, breather line, breather kinky, lump and rogue wave solutions [5-12]. For investigating the characteristics of solitary waves, there are various reliable and fruitful approaches such as inverse scattering scheme [13], tanh function method [14], exp-function method [15,16], Darboux method [17], direct algebraic method [18], first integral

* Corresponding author.
E-mail addresses: harun_math@pust.ac.bd (H.-O. Roshid), mawx@cas.usf.edu (W.-X. Ma).

https://doi.org/10.1016/j.cjph.2020.10.009
Received 11 April 2020; Received in revised form 12 September 2020; Accepted 25 October 2020
Available online 28 October 2020

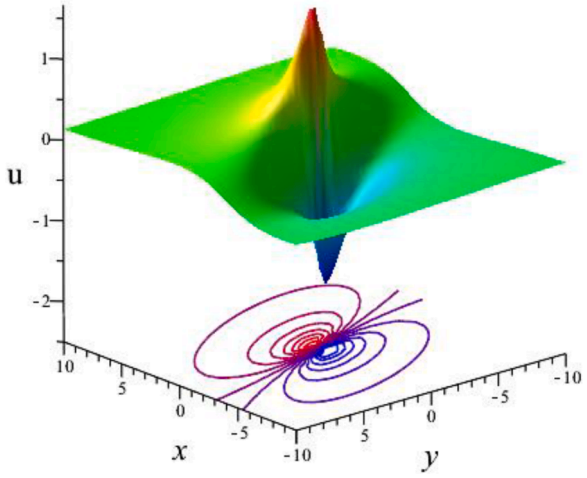

Fig. 1.. (Color online) Outlook of lump wave solution u_1 of the Eq. (6) (For interpretation of the references to color in the text, the reader is referred to the web version of this article.).

method [19, 20], exp $(-\phi(\xi))$expansion method [21], Hirota's bilinear method [22-24] etc. Though, soliton should have elastic property yet fission-fusion type non-elastic properties have been existed in few nonlinear models and investigated by many researchers [12, 23-25].

In mathematical physics, the interaction of rogue wave with other soliton/periodic wave is a kind of remarkable task in nonlinear sciences which are localized both in position and time, while lump wave is localized in every spaces only. Recently, combination of positive quadratic polynomial functions with the exponential/trigonometric functions i.e. collision of kink, lump, rogue and periodic waves produce kinky-lump, kinky-rogue, periodic-lump wave, periodic-rogue waves and kinky-periodic rogue wave for the NLEEs and their nonlinear dynamics concerned a lot of interest [26-41]. In the existed literature, we observed that interactions as mixed lump-kink [27, 28], lump solitons and the interaction phenomena [29-36], lump-stripe soliton solutions [37-38], non-elastic fusion phenomena of multi-solitons [39], N th-order rogue waves [40], two lump solitons [41] are studied by recent dynamical researchers. But it is still unexplored that both bright and dark kinks give the fission phenomena even produce hybrid lump waves, double kinky-periodic-lump type wave exhibits as hybrid lump wave, fission and fusion properties exist in presence and without presence of sinusoidal function and produces hybrid lump waves, both fission-fusion phenomena occurrences in both x-and y-periodic lump waves into a double kink wave and produce hybrid lump waves, annihilations of lump-kink wave.

Motivated by the above works and new properties, we would like to derive novel higher order collision solutions which are not reported in the previous literature for the (3 + 1)-dimensional classical STOL equation [42, 43]:

$$\begin{aligned} &u_t + a\left[\left(3uu_x + u^3\right)_x + u_{xxx}\right] + b\left[\left(2uu_y + u_x\partial_x^{-1}u_y + u^2\partial_x^{-1}u_y\right)_x + u_{xxy}\right] \\ &+c\left[\left(2uu_z + u_x\partial_x^{-1}u_z + u^2\partial_x^{-1}u_z\right) + u_{xxz}\right] = 0. \end{aligned} \tag{1}$$

with real function $u(x,y,z,t)$and real constants a,b,c. Here ∂_x^{-1}indicate integral operator and inverse of ∂_x.

In this article, our main goal is to construct more novel exact collision among lump, periodic and kinky wave solutions that degenerate into periodic line breather waves, kinky periodic waves, double kinky periodic waves, periodic lump waves, double kinky lump waves, kinky periodic lump waves, hybrid lump waves and fission fusion properties of the Eq. (1).

2. Interaction solutions and dynamics of the solutions for STOL equation

Through the relation $u = (\ln f)_x$, the Eq. (1)can be expressed as the form

$$aff_{xxxx} + bff_{xxxy} + cff_{xxxz} - af_xf_{xxx} - bf_xf_{xxy} - cf_xf_{xxz} + ff_{xt} - f_xf_t = 0, \tag{2}$$

with real function $f(x,y,z,t)$to be determined. When $f$satisfies Eq. (2), $u = (\ln f)_x$directly generates a solution of the main Eq. (1).

In order to evaluate $f$explicitly, we assume an ansatz of the following form

$$\begin{aligned} f &= (m_1x + m_2y + m_3z + m_4t + m_5)^2 + (m_6x + m_7y + m_8z + m_9t + m_{10})^2 \\ &+m_{11} + l_1\cos(m_{12}x + m_{13}y + m_{14}z + m_{15}t + m_{16}) \\ &+l_2\cosh(m_{17}x + m_{18}y + m_{19}z + m_{20}t + m_{21}), \end{aligned} \tag{3}$$

where $m_1, m_2, m_3, \ldots\ldots m_{16}$, $l_1$and $l_2$are real free constants, $m_{17}, \ldots\ldots m_{21}$are real/completely imaginary constants. Inserting Eq. (3) to Eq. (2), collect every coefficients of $x,y,z,t,\cos,\sin,\cosh,\sinh$together and setting each of these expression equal to zero, we gain a system of equations in $m_1, m_2, m_3, \ldots\ldots m_{21}$, $l_1$and l_2. Solving this system of algebraic equations by using Maple 18, we obtain the following four

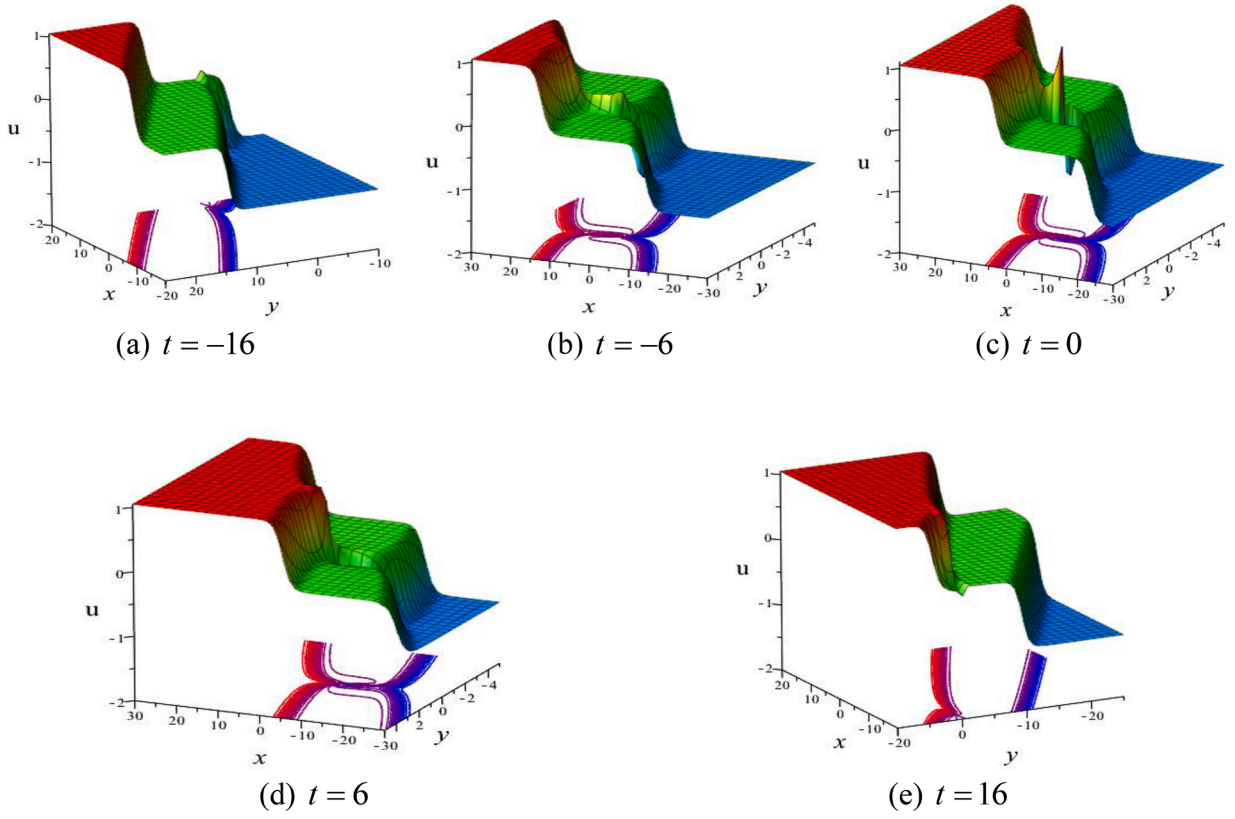

Fig. 2.. (Color online) Fission-fusion profiles of the lump wave get into a duel kinky waves for the solutions Eq. (9) with $l_2 = a = b = 1, c = -1, m_1 = 3, m_2 = -146, m_3 = -4.4, m_5 = 4, m_6 = 3, m_7 = -3.9, m_8 = 10.24, m_{10} = 1, m_{11} = 8.82, m_{17} = 1.05, m_{18} = 2.1, m_{19} = 4.6, m_{21} = 0$at $z = 0$(For interpretation of the references to color in the text, the reader is referred to the web version of this article.).

results,

Case 1:

$$l_1 = 0, l_2 = 0, m_4 = 0, m_9 = 0, \quad m_i = m_i (i = 1, 2, 3, 5, 6, 7, 8, 10, 11, \cdots, 21). \tag{4}$$

Inserting Eq. (4) into the Eq. (3), we obtain

$$f = (m_1 x + m_2 y + m_3 z + m_5)^2 + (m_6 x + m_7 y + m_8 z + m_{10})^2 + m_{11}. \tag{5}$$

Using the relation $u = (\ln f)_x$, Eq. (5)offers the result

$$u_1 = [2(m_1 x + m_2 y + m_3 z + m_5)m_1 + 2(m_6 x + m_7 y + m_8 z + m_{10})m_6]/ \left[(m_1 x + m_2 y + m_3 z + m_5)^2 + (m_6 x + m_7 y + m_8 z + m_{10})^2 + m_{11}\right]. \tag{6}$$

The result Eq. (6) contains nine free arbitrary constants and exhibits lump wave with the condition $m_{11} > 0$ in the xyplane. The line soliton solution that is definitely dissimilar starting a moving line soliton, arise very quickly and disappear in the constant background within tiny time but in the intermediate time it gives highest peak. It is well known that $u \to 0$as the two quadratic functions tend to positive or negative infinity. It maximum minimum amplitude occurs at the points $\left(\frac{m_2 m_{10} - m_5 m_7}{m_1 m_7 - m_2 m_6} \pm \sqrt{\frac{m_{11}}{{m_1}^2 + {m_6}^2}}, \frac{m_5 m_6 - m_1 m_{10}}{m_1 m_7 - m_2 m_6}\right)$when $z = 0$. The Fig.1 represents stretch of the lump wave solution Eq. (6), consists of one deep hole and one high crest for the particular values $m_1 = 2$, $m_2 = 3, m_3 = 2, m_5 = 1, m_6 = 5, m_7 = 1, m_8 = 5, m_{10} = 1, m_{11} = 10$, in the xyplane with $t = 0, z = 0$. The peak of the lump wave locates at $\left(-\frac{2}{13} + \frac{\sqrt{290}}{29}, -\frac{3}{13}\right)$, the valley locates at $\left(-\frac{2}{13} - \frac{\sqrt{290}}{29}, -\frac{3}{13}\right)$and maximum amplitude is $\frac{\sqrt{290}}{10}$and deep is equal distance i.e. $-\frac{\sqrt{290}}{10}$.

Case 2:

$$\begin{aligned} &l_1 = 0, m_4 = 0, m_9 = 0, \; m_{20} = -m_{17}^2 (a m_{17} + b m_{18} + c m_{19}) \\ &l_2 = l_2, m_i = m_i \, (i = 1, 2, 3, 5, 6, 7, 8, 10, 11, 17, 18, 19, 21), \end{aligned} \tag{7}$$

where $a, b$and $c$can take arbitrary values.

Inserting Eq. (7) into the Eq. (3), we emerge to

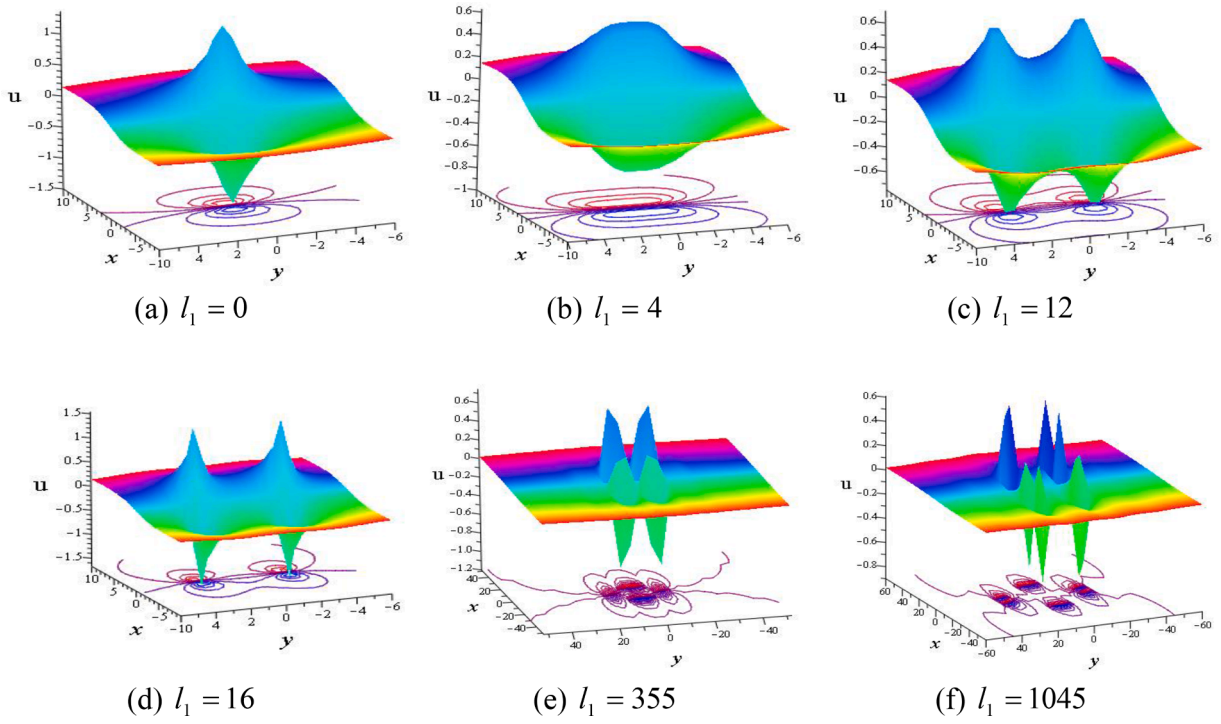

Fig. 3.. (Color online) Diagrams of collision solution $u_3$of Eq. (12) for the values $a = 3, b = 3, c = -4, m_1 = -1, m_2 = 1, m_3 = -2, m_5 = -0.1, m_6 = 1, m_7 = 1, m_8 = 2, m_{10} = 0.1, m_{11} = 1, m_{12} = 0, m_{13} = 1, m_{14} = -2, m_{16} = 0$(For interpretation of the references to color in the text, the reader is referred to the web version of this article.).

$$f = (m_1x + m_2y + m_3z + m_5)^2 + (m_6x + m_7y + m_8z + m_{10})^2 + m_{11} + l_2\cosh\{m_{17}x + m_{18}y + m_{19}z - m_{17}^2(am_{17} + bm_{18} + cm_{19})t + m_{21}\}. \tag{8}$$

Using the relation $u = (\ln f)_x$, Eq. (8)provides the result

$$u_2 = \begin{bmatrix} 2(m_1x + m_2y + m_3z + m_5)m_1 + 2(m_6x + m_7y + m_8z + m_{10})m_6 \\ +l_2m_{17}\sinh\{m_{17}x + m_{18}y + m_{19}z - m_{17}^2(am_{17} + bm_{18} + cm_{19})t + m_{21}\} \end{bmatrix} / \begin{bmatrix} (m_1x + m_2y + m_3z + m_5)^2 + (m_6x + m_7y + m_8z + m_{10})^2 + m_{11} \\ +l_2\cosh\{m_{17}x + m_{18}y + m_{19}z - m_{17}^2(am_{17} + bm_{18} + cm_{19})t + m_{21}\} \end{bmatrix}. \tag{9}$$

In the solutions Eq. (9), we explore collision of the lump and a double kink waves through demonstration of the Fig. 2. It is seen that only a double kink waves is visible in Fig. 2(a) at the time $t = -16$and a small wave initiate at the lower kink (see from contour plot of Fig. 2(a)) but in its propagation a lump wave come out at the time $t = -6$from the lower kink (see Fig. 2(b)). So, the fission phenomenon of lower kink is happened. As time goes, it moves to the upper kink and then get highest amplitude at $t = 0$as well as lump reach in the middle of the two kinks (see Fig. 2(c)). After then the lump wave goes to the upper kink and amplitude of lump decreases again as time increases (see Fig. 2(d)) and finally diminished to the upper kink at $t = 16$(see Fig. 2(e)). So, the fusion phenomenon of upper kink is occurred. From the overall observation, we see the height of the double kink waves remain same in the overall propagation before and after the collision.

Case 3:

$$\begin{aligned} &l_2 = 0, m_4 = 0, m_9 = 0, m_{15} = m_{12}^2(am_{12} + bm_{13} + cm_{14}) \\ &l_1 = l_1, m_i = m_i\,(i = 1, 2, 3, 5, 6, 7, 8, 10, 11, 12, 13, 14, 16), \end{aligned} \tag{10}$$

where $a, b$and $c$can take arbitrary real values.

Setting Eq. (10) to the Eq. (3), we acquire

$$f = (m_1x + m_2y + m_3z + m_5)^2 + (m_6x + m_7y + m_8z + m_{10})^2 + m_{11} + l_1\cos\{m_{12}x + m_{13}y + m_{14}z + m_{12}^2(am_{12} + bm_{13} + cm_{14})t + m_{16}\}. \tag{11}$$

Using the relation$u = (\ln f)_x$, Eq. (11)offers the result

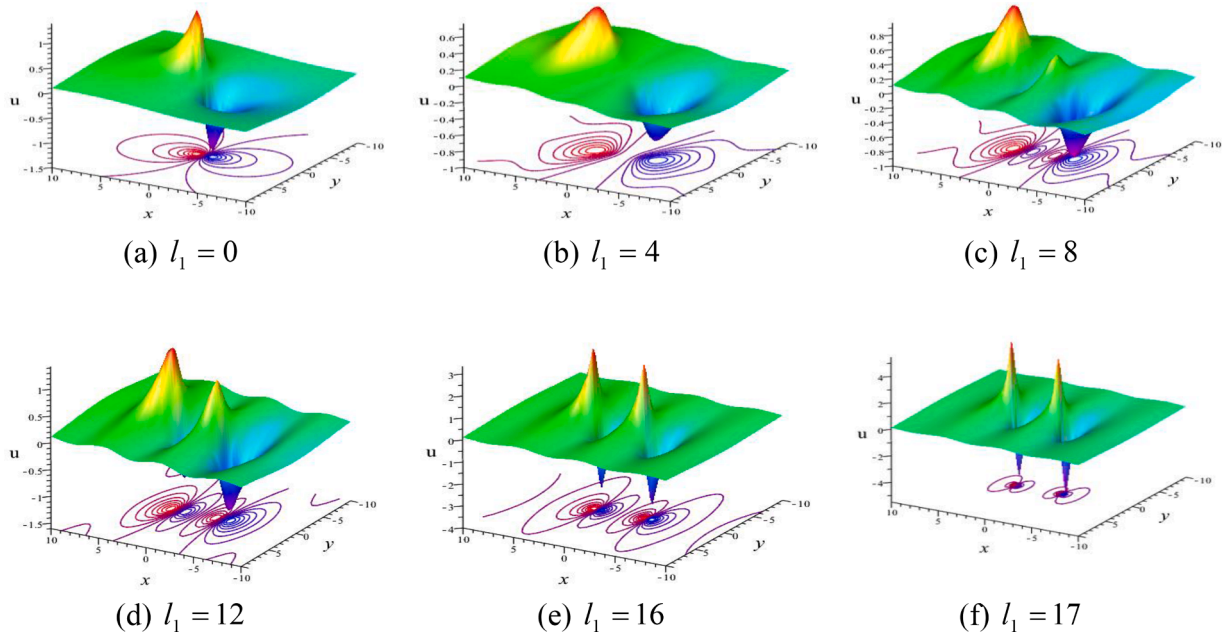

Fig. 4.. (Color online) Diagrams of the collision solution $u_3$of Eq. (12) for the values $a = 3, b = 3, c = -4,\ m_1 = -1, m_2 = 1, m_3 = -2, m_5 = -0.1, m_6 = 1, m_7 = 1, m_8 = 2, m_{10} = 0.1, m_{11} = 1, m_{12} = 1, m_{13} = 0, m_{14} = -2, m_{16} = 0$(For interpretation of the references to color in the text, the reader is referred to the web version of this article.).

$$u_3 = \begin{bmatrix} 2(m_1x + m_2y + m_3z + m_5)m_1 + 2(m_6x + m_7y + m_8z + m_{10})m_6 \\ -l_1 m_{12}\sin\{m_{12}x + m_{13}y + m_{14}z + m_{12}^2(am_{12} + bm_{13} + cm_{14})t + m_{16}\}m_{12} \end{bmatrix} / \begin{bmatrix} (m_1x + m_2y + m_3z + m_5)^2 + (m_6x + m_7y + m_8z + m_{10})^2 + m_{11} \\ +l_1\cos\{m_{12}x + m_{13}y + m_{14}z + m_{12}^2(am_{12} + bm_{13} + cm_{14})t + m_{16}\} \end{bmatrix}. \tag{12}$$

For $l_1 = 0$, $u_3$reduces to single lump only like **case-1** but for $l_1 \neq 0$, $u_3$comes in-terms of two quadratic polynomials and a sinusoidal function (i.e. collision of lump and periodic wave), as depicted in the Figs. 3–5. Here, three sub cases are arising in the followings.

(i) When $m_{12} = 0$and $m_{13} \neq 0$, $u_3$reduces to collision solution with following dynamics:

It is well-known that the lump form with a crest and a trough (observe Fig. 3(a)). But as the value of $l_1$increases, the collision of lump and periodic waves create a fission of lump wave i.e. a crest and a trough progressively split into two crests and two troughs having the same height (observe Fig. 3(b)–3(d)) and propagate along y-direction initially. Thus the fission of lump wave is happened. We also observe that fission of the lump wave is continuous process as for large values of $l_1 = 355$, the lump wave again generate fission and split into four lump waves propagate along both in the $x$and y-directions, even if for $l_1 = 1045$, it gives six lump (hybrid lump) waves (see Fig.3(e, f)) and so on.

(ii) When $m_{12} \neq 0$and $m_{13} = 0$, $u_3$reduces to collision solution with following dynamics:

It gives the similar collision solution (fission of lump) in the figures Fig. 4(b)–4(f) and produces more lump waves propagate periodically toward the x-axis and also the extreme amplitude of the crests and the troughs gradually enlarges as $l_1$increases. In contrast the Fig. 3 with Fig. 4, we observe that the lump wave in the collision solution locates toward the y-axis in Fig. 3but the lump wave in the collision solution locates toward the x-axis in the Fig. 4.

(iii) When $m_{12} \neq 0$and $m_{13} \neq 0$, $u_3$reduces to collision solution with following dynamics:

In fact, some interesting phenomenon can also be observed when both $m_{12} \neq 0$and $m_{13} \neq 0$and the value of coefficient $l_1$increases the trigonometric function that dominate on the values of coefficients in quadratic functions (lump wave) as depicted in Fig. 5(a)-(d). We display the corresponding 3D plot (3D as in upper and contour plot as in lower), density and 2D profile in the xyplane (for $y = -3, 0, 3$in Fig. 5(c)) of the lump-periodic wave. Anyone can see that at $y = 0$amplitude of the lump gives highest peak (observe Fig. 5(c)). On the other hand, another periodic-rogue wave can be observed in xtplane as in the Fig. 5(d).

Case 4:

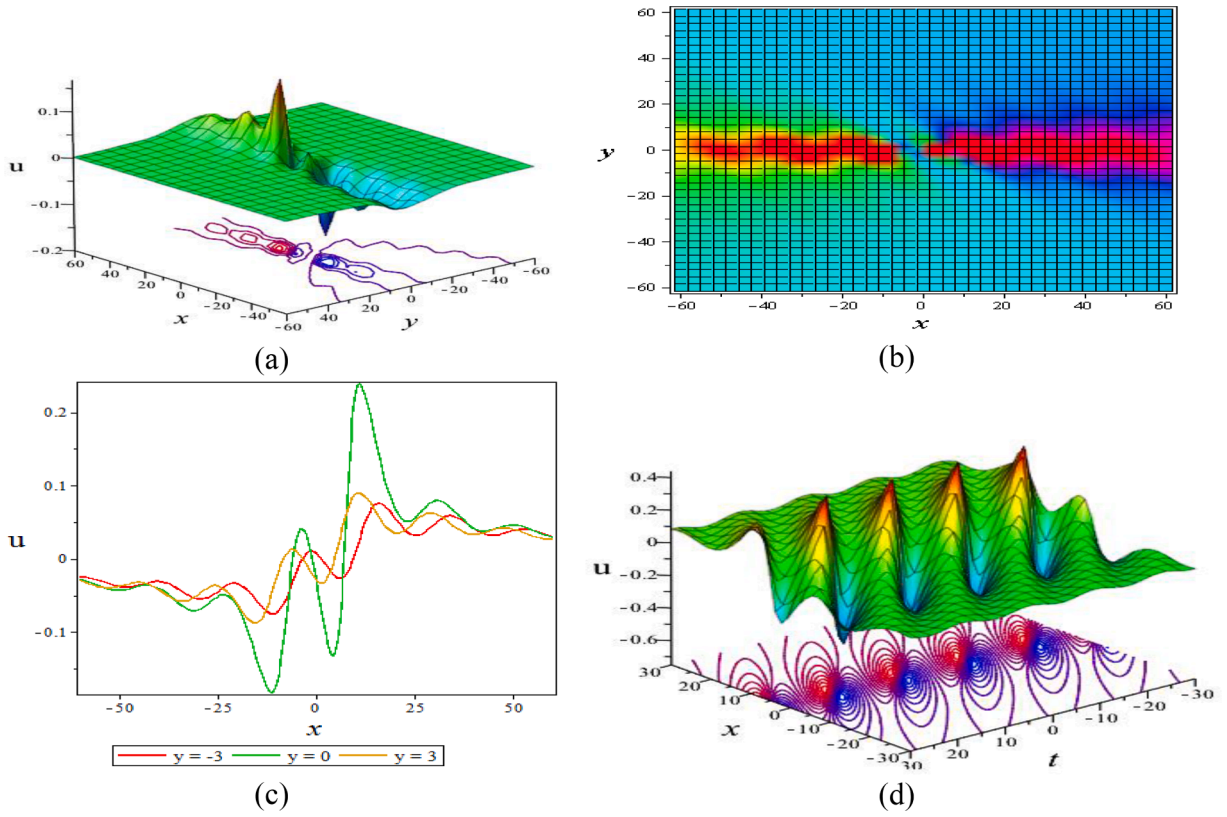

Fig. 5.. (Color online) Profile of the collision of lump and periodic waves solution $u_3$of Eq. (12) for $l_1 = 15, a = 1, b = 2, c = -4, m_1 = 0.5, m_2 = -1, m_3 = 1, m_5 = -0.5, m_6 = -0.25, m_7 = -3, m_8 = -3.5, m_{10} = 1, m_{11} = 20, m_{12} = \frac{1}{3}, m_{13} = \frac{4}{15}, m_{14} = -0.8, m_{16} = 0$: (a) the 3D plot, (b) the density plot and (c) the similar curve plot at $z = 0, t = 0$; (d) Periodic rogue wave at $z = 0, y = 0$(For interpretation of the references to color in the text, the reader is referred to the web version of this article.).

$$\begin{aligned} &m_4 = 0, m_9 = 0, m_{15} = m_{12}^2(am_{12} + bm_{13} + cm_{14}), m_{20} = -m_{17}^2(am_{17} + bm_{18} + cm_{19}) \\ &l_1 = l_1, l_2 = l_2, m_i = m_i\ (i = 1, 2, 3, 5, 6, 7, 8, 10, 11, 12, 13, 14, 16, 17, 18, 19, 21), \end{aligned} \tag{13}$$

where $a, b$and $c$can take any arbitrary values.

Putting Eq. (13) into the Eq. (3), offers the result

$$\begin{aligned} f = &(m_1x + m_2y + m_3z + m_5)^2 + (m_6x + m_7y + m_8z + m_{10})^2 + m_{11} \\ &+l_1\cos\{m_{12}x + m_{13}y + m_{14}z + m_{12}^2(am_{12} + bm_{13} + cm_{14})t + m_{16}\} \\ &+l_2\cosh\{m_{17}x + m_{18}y + m_{19}z - m_{17}^2(am_{17} + bm_{18} + cm_{19})t + m_{21}\}. \end{aligned} \tag{14}$$

Using the relation$u = (\ln f)_x$, Eq. (14)offers the result

$$\begin{aligned} u_4 = &\begin{bmatrix} 2(m_1x + m_2y + m_3z + m_5)m_1 + 2(m_6x + m_7y + m_8z + m_{10})m_6 \\ -l_1m_{12}\sin\{m_{12}x + m_{13}y + m_{14}z + m_{12}^2(am_{12} + bm_{13} + cm_{14})t + m_{16}\} \\ +l_2m_{17}\sinh\{m_{17}x + m_{18}y + m_{19}z - m_{17}^2(am_{17} + bm_{18} + cm_{19})t + m_{21}\} \end{bmatrix} / \\ &\begin{bmatrix} (m_1x + m_2y + m_3z + m_5)^2 + (m_6x + m_7y + m_8z + m_{10})^2 + m_{11} \\ +l_1\cos\{m_{12}x + m_{13}y + m_{14}z + m_{12}^2(am_{12} + bm_{13} + cm_{14})t + m_{16}\} \\ +l_2\cosh\{m_{17}x + m_{18}y + m_{19}z - m_{17}^2(am_{17} + bm_{18} + cm_{19})t + m_{21}\} \end{bmatrix}. \end{aligned} \tag{15}$$

In the solution Eq. (15), comes in terms of two quadratic polynomials, a periodic and a hyperbolic function which exhibits double kinky-periodic-lump type wave propagation for$l_2 \neq 0,\ l_1 \neq 0$. In this case, three clusters are arising in the followings.

Cluster-1 - Taking $l_2$very small as$l_2 \to 0$:

Taking $l_2$very small, a dynamical situation viewed in the Figs.6–7 for the values $a = 5, b = 1, c = -1, m_3 = m_5 = m_8 = m_{10} = m_{11} = m_{14} = 1, m_{16} = 0.1, m_{19} = 7, m_{21} = 1$at $z = 0$. The solution $u_4$provides double kinky-periodic lump wave in which some$x$-periodic-

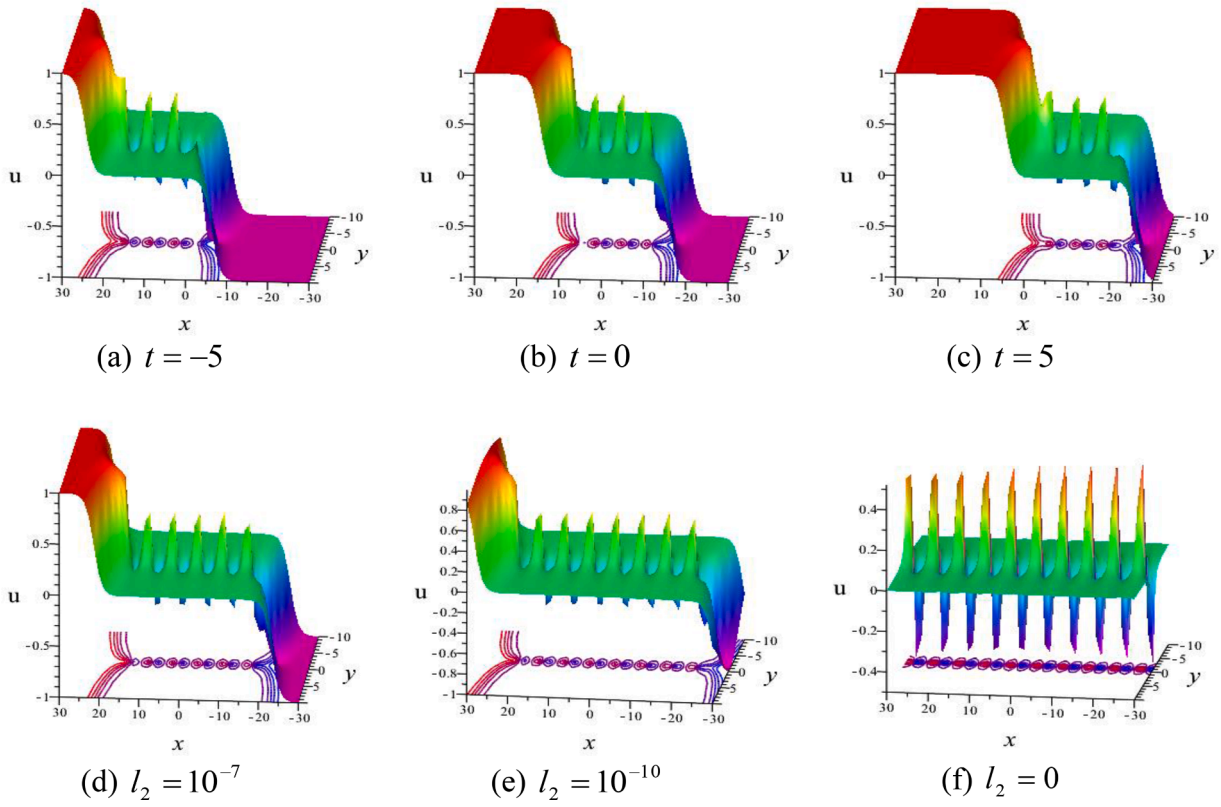

Fig. 6.. (Color online) Profiles of collision solution $u_4$of Eq. (15) for the parameters $m_1=m_6=m_{13}=m_{18}=0, m_2=m_7=m_{12}=m_{17}=1, l_1=0.5$: (a)-(c) the periodic lump get into the double kinky wave for $l_2=10^{-4}$; (d)-(e) increases of periodic lump into the double kinky wave for $l_2\to 0$; (f) x- periodic lump wave for $l_2=0$(For interpretation of the references to color in the text, the reader is referred to the web version of this article.).

lump with period $2\pi/m_{12}$get into the double kink and kinky wave moves through $x$axis with time increases for the values as depicted in the Fig. 6(a)-(c). In this case number of lump wave remains same with the same value of $l_2=0.0001$. But when$l_2\to 0$, the number of lump wave gradually increases as the values of $l_2$decreases (observe Fig. 6(d)-(e)), even if, kink vanishes and only periodic lump exist for $l_2=0$(observe Fig. 6(f)) at $t=0$.Actually, changing different parametric constraint of the solution Eq. (15) distinguish characteristics again exhibits in Fig. 7(a)-(d) as $y-$ periodic lump with period $2\pi/m_{13}$get into the kink that arises with a constant background and decay go back to the same previous background at a longer time. On the other hand, same behavior can be observed in line soliton in the Fig. 7(e)-(h). Interesting characteristics can also be experienced when constant coefficients vanishes (i.e., $m_5=m_{10}=m_{11}=m_{16}=m_{21}=0$) as depicted in the Fig.8(a)-(c) that behaved $y-$ periodic bright-dark lump waves get into the double kink waves with period $2\pi/m_{13}$. The bright lumps get into the lower kink and dark lumps get into the upper kink. Both kinks give the fission phenomena and produce hybrid lump waves in which height and number of lump increases as $l_1$increase (observe Fig. 8(a)-(c)). These novel nonlinear phenomena are the first reported for the $(3+1)$-dimension STOL equation.

Cluster-2 - Taking $l_2$not so small:

Taking $l_2$not so small, a dynamical situation viewed to the solutionu_4, provides double kinky waves in which two lump waves periodically get into the kink waves and exhibits fission fusion phenomena. Solution Eq. (15), exhibits fission-fusion phenomena as depicted in the Figs.9(a)-(f) and 10(a)-(f) which are similar to the fission-fusion phenomena of the Fig. 2. But the only different is that $y$periodic two lumps causes fission from the upper kink and then fused into the lower kink when $m_{12}=0, m_{13}\neq 0$(observe Fig. 9(a)-(e)) and $x$periodic two lumps causes fission from the upper kink and then fused into the lower kink when $m_{12}\neq 0, m_{13}=0$(observe Fig. 10(a)-(f)). Both the figures Figs. 9(a)-(f) and 10(a)-(f) are sketch with specific parameters $l_1=16, l_2=0.5, a=-3, b=2, c=1, m_1=-1, m_2=1, m_3=-2, m_5=0, m_6=1, m_7=1, m_8=4, m_{10}=0, m_{11}=1, m_{14}=1, m_{16}=0, m_{17}=1, m_{18}=0, m_{19}=2, m_{21}=0$at $z=0$. These novel nonlinear phenomenon is the first reported for the $(3+1)$-dimension STOL equation.

Cluster-3 - Taking lump vanish (i.e., $m_i=0; i=1,2,3,5,6,7,10$):

When $m_i=0\,(i=1,2,3,5,6,7,10)$; lump waves being diminished and then collision between the kinky and periodic wave are appeared in the solution Eq. (15), then we find

$$\begin{aligned} f &= m_{11}+l_1\cos\{m_{12}x+m_{13}y+m_{14}z+m_{12}^2(am_{12}+bm_{13}+cm_{14})t+m_{16}\} \\ &\quad +l_2\cosh\{m_{17}x+m_{18}y+m_{19}z-m_{17}^2(am_{17}+bm_{18}+cm_{19})t+m_{21}\}. \end{aligned} \tag{16}$$

The solution Eq. (16) can convert to diverse collision solutions, selecting the constants $m_{17}, m_{18}, m_{19}, m_{21}$are real/purely imaginary

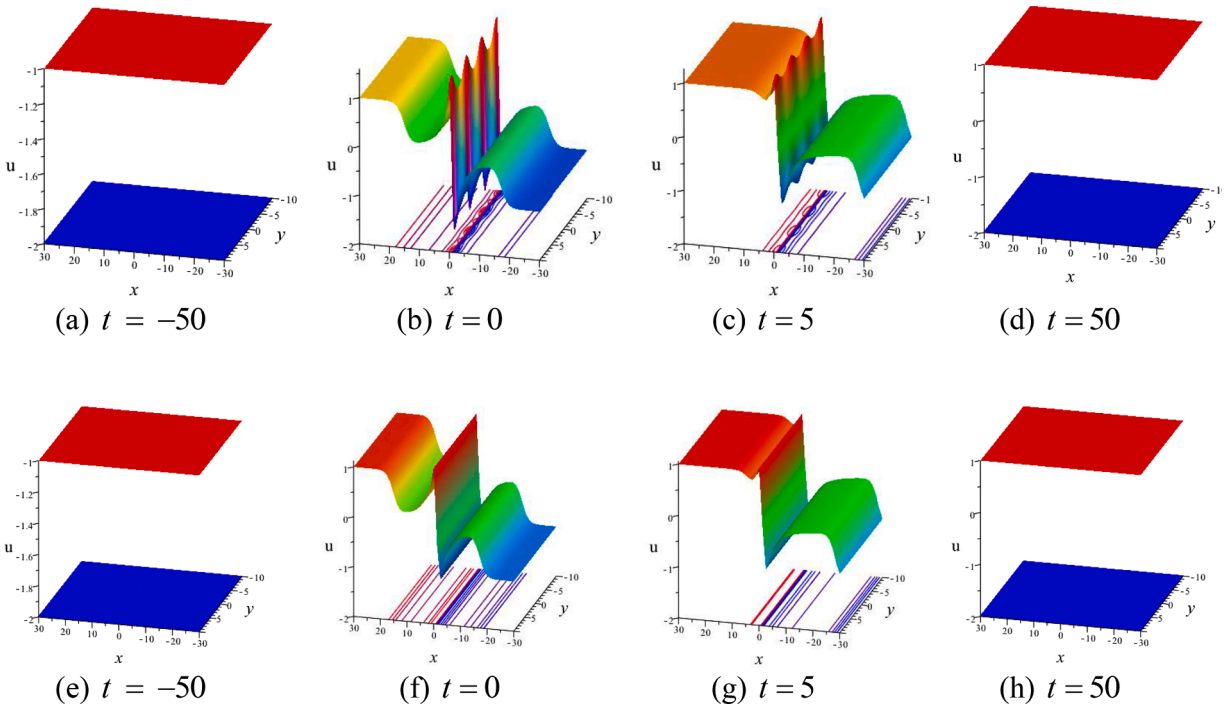

Fig. 7.. (Color online) Annihilation properties of collision solution $u_4$of Eq. (15) for $l_1 = 0.5, l_2 = 10^{-4}$at $z = 0$; (a)-(d) y – periodic lump wave get into the kinky wave for $m_2 = m_7 = m_{12} = m_{18} = 0, m_1 = m_6 = m_{13} = m_{17} = 1$; (e)-(h) x- periodic lump get into the kink wave for $m_2 = m_7 = m_{13} = m_{18} = 0, m_1 = m_6 = m_{12} = m_{17} = 1$(For interpretation of the references to color in the text, the reader is referred to the web version of this article.).

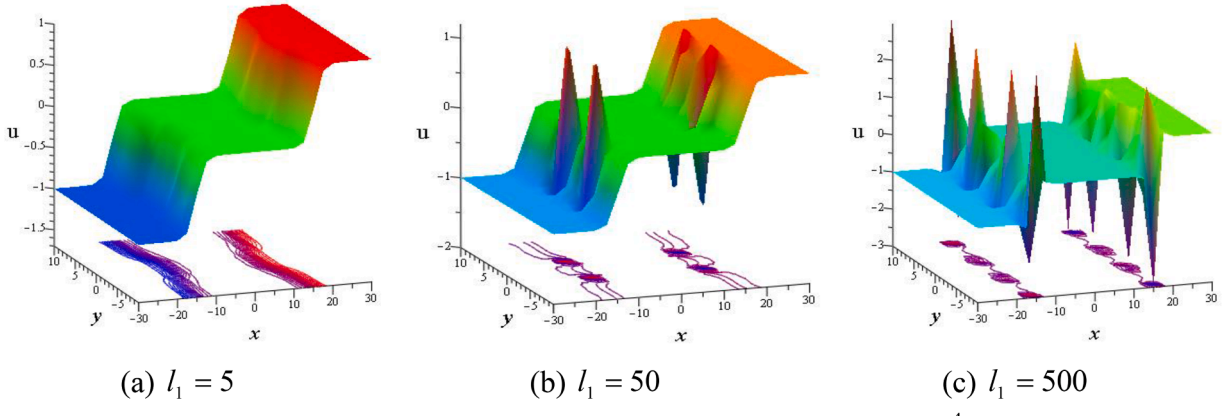

Fig. 8.. (Color online) Profiles of collision solution $u_4$of Eq. (15) for $l_2 = 10^{-4}, a = 5, b = 1, c = -1, m_1 = m_6 = m_{12} = m_{18} = 0, m_{19} = 7, m_2 = m_3 = m_7 = m_8 = m_{13} = m_{14} = m_{17} = 1$at $t = 0, z = 0$(For interpretation of the references to color in the text, the reader is referred to the web version of this article.).

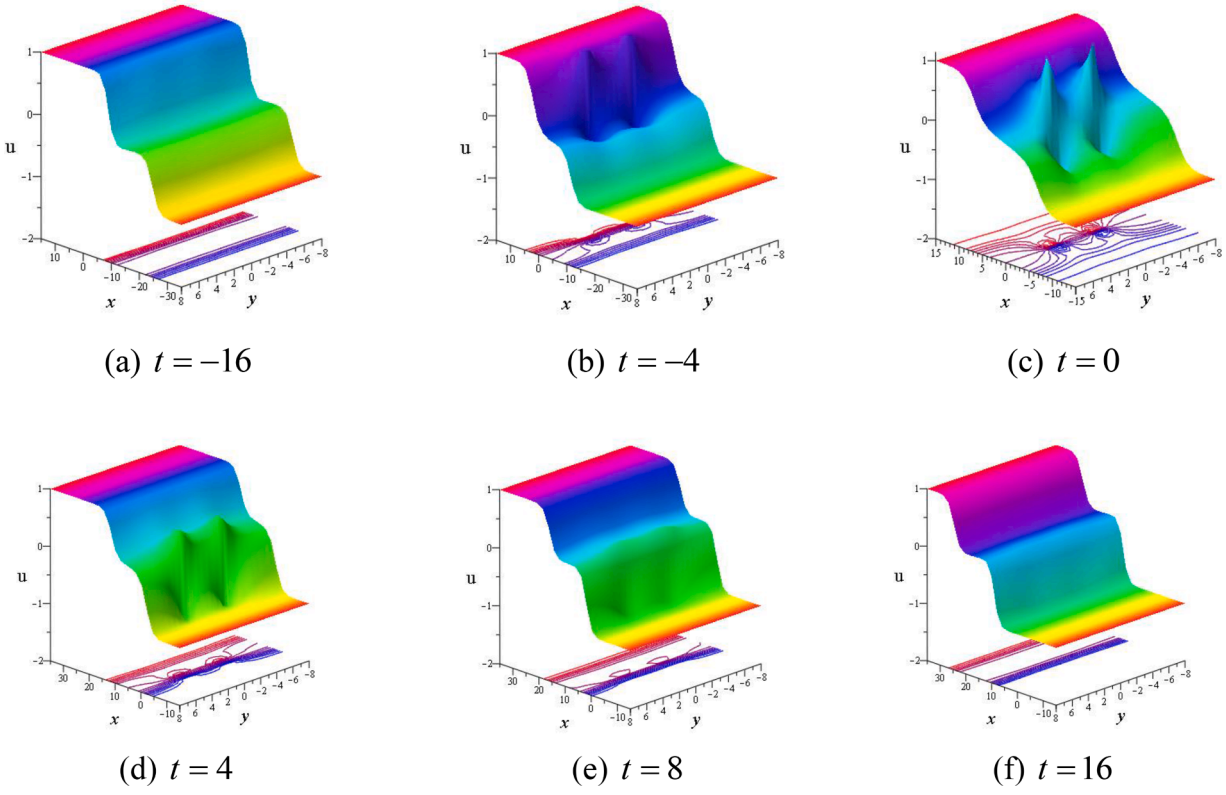

Fig. 9.. (Color online) Fission-fusion profile of y-periodic lump wave with the double kink wave of solution Eq. (15)for $m_{13}=1$(For interpretation of the references to color in the text, the reader is referred to the web version of this article.).

value.

(i) For $m_{17}, m_{18}, m_{19}, m_{21}$are real valued, we acquire a collision wave of the Eq. (1) using the relation $u=(\ln f)_x$as:

$$u_5=\begin{bmatrix}-l_1m_{12}\sin\{m_{12}x+m_{13}y+m_{14}z+m_{12}^2(am_{12}+bm_{13}+cm_{14})t+m_{16}\}\\+l_2m_{17}\sinh\{m_{17}x+m_{18}y+m_{19}z-m_{17}^2(am_{17}+bm_{18}+cm_{19})t+m_{21}\}\end{bmatrix}/$$
$$\begin{bmatrix}m_{11}+l_1\cos\{m_{12}x+m_{13}y+m_{14}z+m_{12}^2(am_{12}+bm_{13}+cm_{14})t+m_{16}\}\\+l_2\cosh\{m_{17}x+m_{18}y+m_{19}z-m_{17}^2(am_{17}+bm_{18}+cm_{19})t+m_{21}\}\end{bmatrix}. \quad (17)$$

Characteristics of the solution $u_5$for the Eq. (17) are explained for diverse choose of the involve parametric values in the figure Fig. 11 and corresponding contour line of the diagram are drawn bellow of the figures in Fig. 11(a)–11(d). For $l_1=0$, $u_5$reduces to double kinky waves (see Fig. 11(a)) but for $l_1\neq 0$, $u_5$is collision of a y- kinky periodic breather wave (see Fig. 11(b)–(d)). Evidently, as $t$changes the collision wave moves toward the $x-$ axis and the phase of the periodic wave changes after $\frac{2\pi}{m_{13}}$along y-axis.

In this case, we also observe that changing different parametric constraint in the solution Eq. (17) distinguish characteristics again exhibits which are periodic line breather waves proceed in various directions as depicted in the Fig. 11(e)-(h), (i)-(l), (m)-(p). Each group of periodic line breather waves begins with a constant background and decay return to the same previous background at a longer time.

(i) For $m_{17}, m_{18}, m_{19}, m_{21}$are pure imaginary valued, i.e., $m_{17}=i\tilde{m}_{17}, m_{18}=i\tilde{m}_{18}, m_{19}=i\tilde{m}_{19}, m_{21}=i\tilde{m}_{21}$with $\tilde{m}_{17}, \tilde{m}_{18}, \tilde{m}_{19}$and $\tilde{m}_{21}$are real valued, we acquire a collision of two breather waves of the Eq. (1) using the relation $u=(\ln f)_x$as:

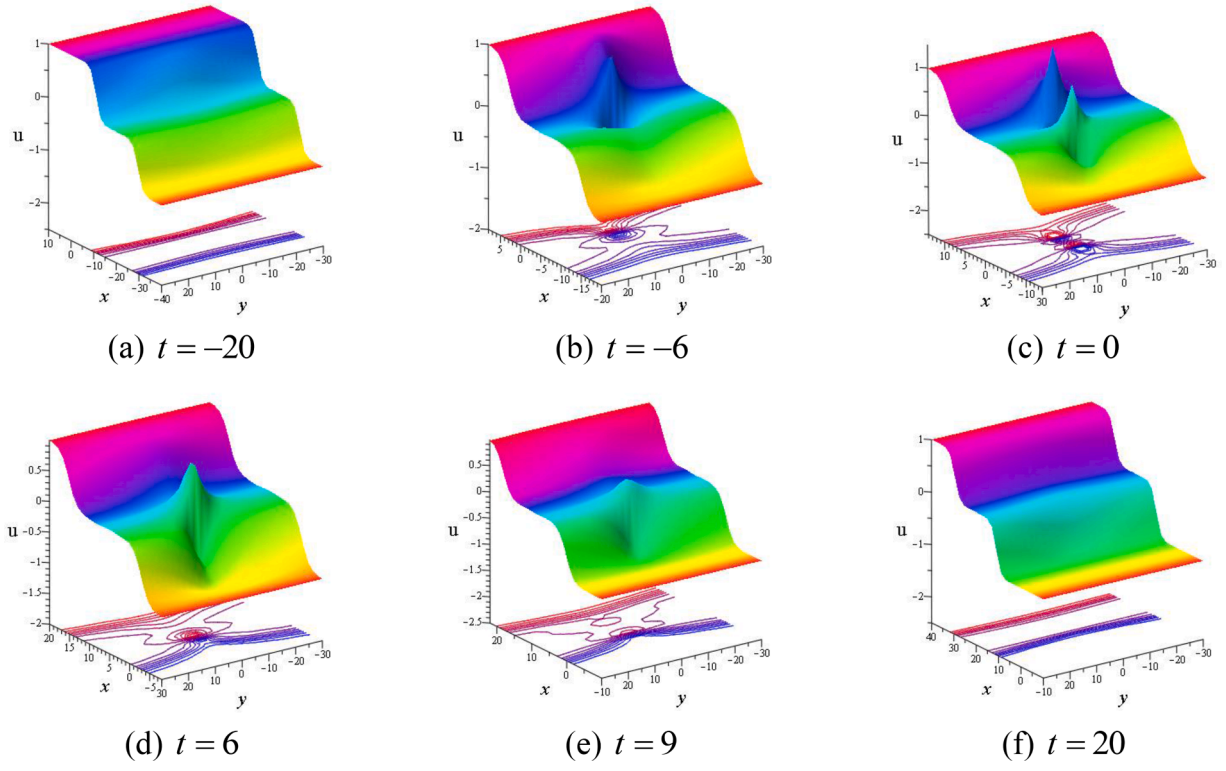

Fig. 10.. (Color online) Fission-fusion profile of x-periodic lump wave with the double kink wave of solution Eq. (15)for $m_{12} = 1$(For interpretation of the references to color in the text, the reader is referred to the web version of this article.).

$$\tilde{u}_5 = \begin{bmatrix} -l_1 m_{12}\sin\{m_{12}x + m_{13}y + m_{14}z + m_{12}^2(am_{12} + bm_{13} + cm_{14})t + m_{16}\} \\ -l_2\tilde{m}_{17}\sin\left\{\tilde{m}_{17}x + \tilde{m}_{18}y + \tilde{m}_{19}z + \tilde{m}_{17}^2\left(a\tilde{m}_{17} + b\tilde{m}_{18} + c\tilde{m}_{19}\right)t + \tilde{m}_{21}\right\} \end{bmatrix} / \begin{bmatrix} m_{11} + l_1\cos\{m_{12}x + m_{13}y + m_{14}z + m_{12}^2(am_{12} + bm_{13} + cm_{14})t + m_{16}\} \\ +l_2\cos\left\{\tilde{m}_{17}x + \tilde{m}_{18}y + \tilde{m}_{19}z + \tilde{m}_{17}^2\left(a\tilde{m}_{17} + b\tilde{m}_{18} + c\tilde{m}_{19}\right)t + \tilde{m}_{21}\right\} \end{bmatrix}. \tag{18}$$

Lastly, the solution represented by Eq. (18) are different periodic waves for different chooses of parameters in $\tilde{u}_5$. When $l_1 = 0$, $\tilde{u}_5$is a one periodic wave that confine in the position and time directions (observe Fig. 12(a)). Otherwise, when $l_1 \neq 0$, then $\tilde{u}_5$exhibits the dual periodic waves in both $xy$and xz- planes (observe Fig. 12(b) and (c)).

3. Conclision

In summary, interaction solutions of the (3 + 1)-dimensional STOL equation have been determined successfully. With the aid of Maple software, a test function is carefully used to derive different nonlinear dynamical properties. As a result, some novel collision solutions among the lump, periodic and kinky waves are derived of the STOL model. We also established fission fusion properties for the collision of lump and kink waves, lump and periodic waves and among the collision of lump, kink and periodic waves. We also observed that fission and fusion properties exist in presence and without presence of sinusoidal function and produces hybrid lump waves. By taking purely imaginary values of some parameters, we derived line breather and double periodic breather wave solutions. To better understand the dynamic natures of the obtained collision solutions, we depict adequate 3d plots and contour diagrams by choosing suitable parametric values with the aid of computational software Maple 18. It is expected that our achieved solutions can improve the dynamical characteristics of the other higher order models.

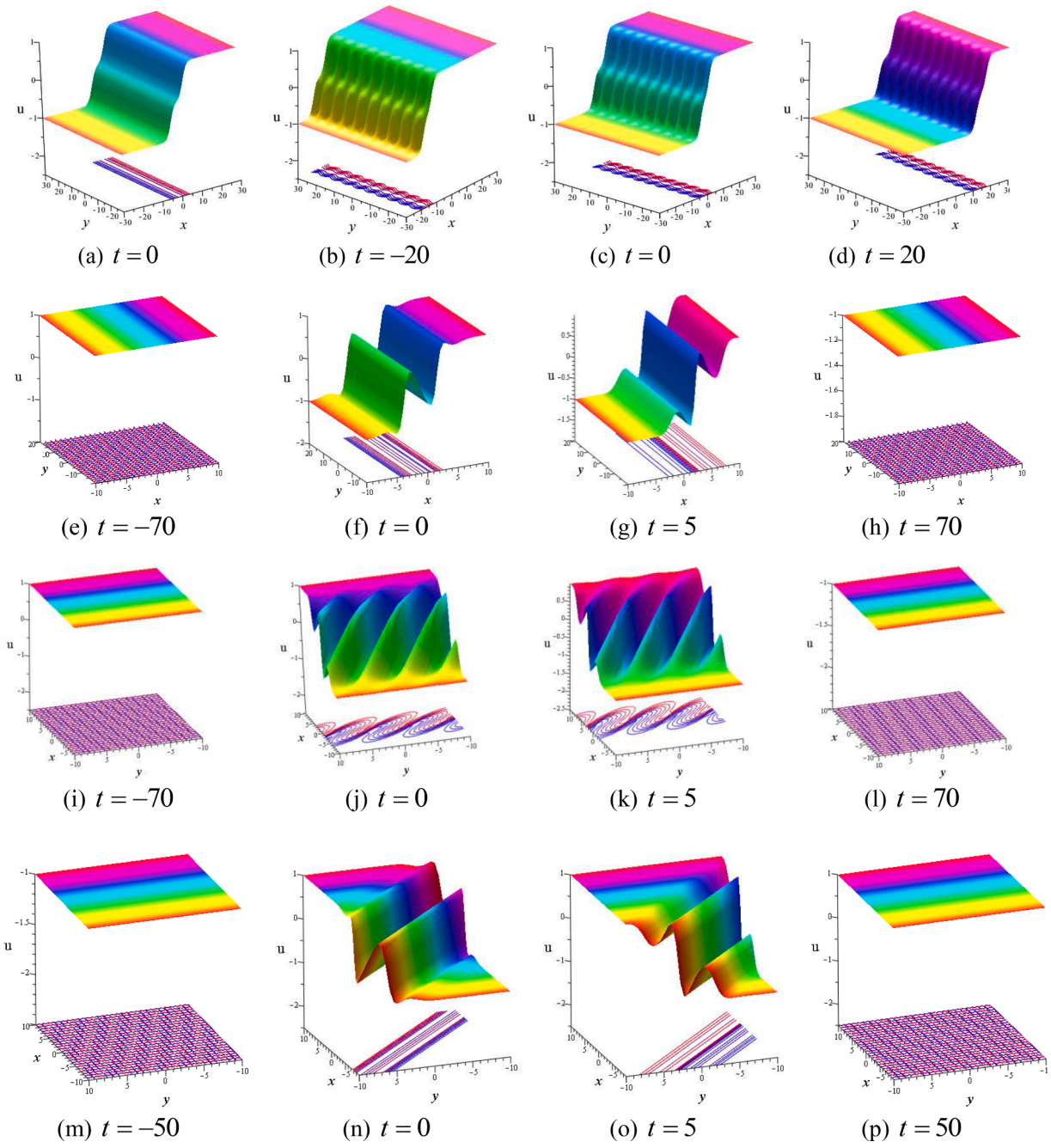

Fig. 11.. (Color online) Annihilation properties of the collision solution u_5 of Eq. (17) for $a=1, b=-2, c=3, m_{11}=1500, m_{14}=-2, m_{16}=1, m_{17}=1, m_{19}=-1/12, m_{21}=1$ and $l_2=100$: (a) double kinky waves for $l_1=m_{12}=m_{18}=0, m_{13}=1$; (b)-(d) y- periodic and double kinky waves for $l_1=1000, m_{12}=m_{18}=0, m_{13}=1$; (e)-(h) x- periodic and double kinky waves for $l_1=1000, m_{13}=m_{18}=0, m_{12}=1$; (i)-(l) (x,y)- periodic and double kinky waves for $l_1=1000, m_{18}=0, m_{12}=m_{13}=1$; (m)-(p) (x,y)- periodic and double kinky waves for $l_1=1000, m_{12}=m_{13}=m_{18}=1$(For interpretation of the references to color in the text, the reader is referred to the web version of this article.).

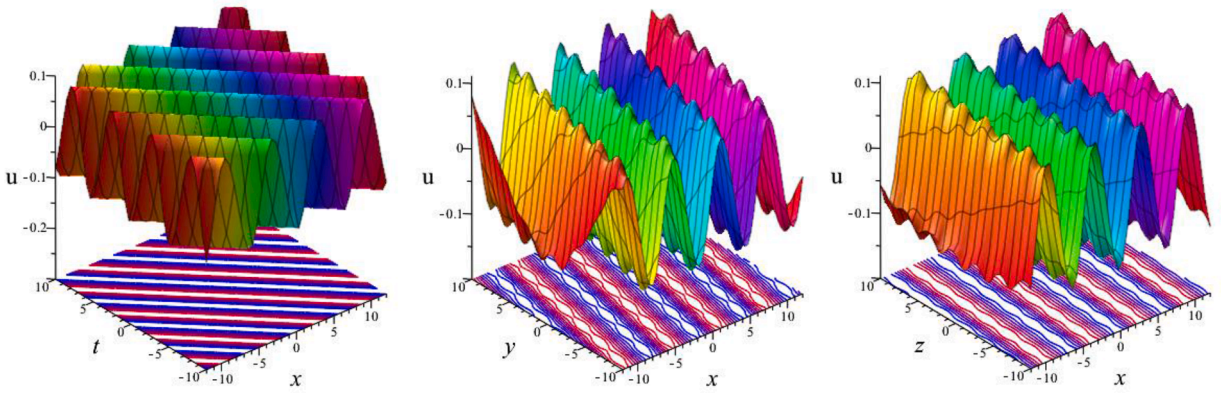

Fig. 12.. (Color online) Diagrams of the collision solution $\tilde{u}_5$of Eq. (18) for $a = -1, b = 1, c = -0.6, m_{11} = 1, m_{12} = 0, m_{13} = 2, m_{14} = -2, m_{16} = 1, l_2 = 0.1$ and $\tilde{m}_{17} = 1, \tilde{m}_{18} = -0.25, \tilde{m}_{19} = -1/12, \tilde{m}_{21} = 1$: (a) one periodic wave at $l_1 = 0$; (b)-(c) dual periodic wave at $l_1 = 0.1$(For interpretation of the references to color in the text, the reader is referred to the web version of this article.).

Declaration of Competing Interest

The researchers have no conflict of interest.

References

[1] A.R. Seadawy, Stability analysis for Zakharov-Kuznetsov equation of weakly nonlinear ion-acoustic waves in a plasma, Comput. Math. Appl. 67 (2014) 172–180.
[2] H. Triki, A. Biswas, S.P. Moshokoa, M. Belic, Optical solitons and conservation laws with quadratic-cubic nonlinearity, Optik 128 (2017) 63–70.
[3] B.Q. Li, Y.L. Ma, Periodic solutions and solitons to two complex short pulse (CSP) equations in optical fiber, Optik 144 (2017) 149–155.
[4] H.W. Yang, X. Chen, M. Guo, Y.D. Chen, A new ZK-BO equation for three-dimensional algebraic Rossby solitary waves and its solution as well as fission property, Nonlinear Dynam. 91 (2018) 2019–2032.
[5] W.Q. Peng, S.F. Tian, T.T. Zhang, Dynamics of the soliton waves, breather waves, and rogue waves to the cylindrical Kadomtsev-Petviashvili equation in pair-ion-electron plasma, Phys. Fluid 31 (2019), 102107.
[6] W.Q. Peng, S.F. Tian, X.B. Wang, T.T. Zhang, Y. Fang, Riemann-Hilbert method and multi-soliton solutions for three-component coupled nonlinear Schrödinger equations, J. Geom. Phys. 146 (2019), 103508.
[7] L.D. Zhang, S.F. Tian, W.Q. Peng, T.T. Zhang, X.J. Yan, The dynamics of lump, lump-off and rogue wave solutions of (2+1)-dimensional Hirota-Satsuma-Ito equations, East Asian J. Appl. Math. 10 (2020) 243–255.
[8] W.Q. Peng, S.F. Tian, T.T. Zhang, Y. Fang, Rational and semi-rational solutions of a nonlocal (2+ 1)-dimensional nonlinear Schrödinger equation, Math. Meth. Appl. Sci. 42 (2019) 6865–6877.
[9] A.C. Cevikel, A. Bekir, New solitons and periodic solutions for (2+1)-dimensional Davey-Stewartson equations, Chin. J. Phys. 51 (1) (2013) 1–13.
[10] A. Bekir, M. Kaplan, Exponential rational function method for solving nonlinear equations arising in various physical models, Chin. J. Phys. 54 (3) (2016) 365–370.
[11] E. Tala-Tebue, H. Rezazadeh, M. Eslami, A. Bekir, New approach to model coupled nerve fibers and exact solutions of the system, Chin. J. Phys. 62 (2019) 179–186.
[12] M.S. Ullah, H.O. Roshid, M.Z. Ali, Z. Rahman, Dynamical structures of multi-soliton solutions to the Bogoyavlenskii's breaking soliton equations, Eur. Phys. J. Plus 135 (2020) 282.
[13] M.J. Ablowitz, M.A. Ablowitz, P.A. Clarkson, Solitons, Nonlinear Evolution Equations and Inverse Scattering, Cambridge university press, 1991.
[14] A.M. Wazwaz, The tanh method for traveling wave solutions of nonlinear equations, Appl. Math. Comput. 154 (2004) 713–723.
[15] X.H. Wu, J.H. He, Exp-function method and its application to nonlinear equations, Chaos, Solitons and Fractals 38 (2008) 903–910.
[16] A. Bekir, Application of the Exp-function method for nonlinear differential-difference equations, Appl. Math. Comput. 215 (11) (2010) 4049–4053.
[17] V.B. Matveev, M.A. Salle, Darboux Transformation and Solitons, Springer-Verlag, Berlin, 1991.
[18] R. Hirota, Direct Methods in Soliton Theory, Cambridge University Prees, 2004.
[19] Z. Feng, The first-integral method to study the Burgers–Korteweg–de Vries equation, J. Phys. A: Math. Gen. 35 (2002) 343–349.
[20] A. Bekir, Ö. Ünsal, Analytic treatment for nonlinear evolution equations by using first integral method, Pramana – J. Phys. 79 (1) (2012) 3–17.
[21] H.O. Roshid, M.A. Rahman, The exp (− Φ (η))-expansion method with application in the (1+ 1)-dimensional classical Boussinesq equations, Result Phys. 4 (2014) 150–155.
[22] M.B. Hossen, H.O. Roshid, M.Z. Ali, Characteristics of the solitary waves and rogue waves with interaction phenomena in a (2+ 1)-dimensional Breaking Soliton equation, Phys. Lett. A 382 (2018) 1268–1274.
[23] S. Wang, X.Y. Tang, S.Y. Lou, Soliton fission and fusion: burgers equation and Sharma-Tasso-Olver equation, Chaos, Solitons and Fractals 21 (2004) 231–239.
[24] A.H. Chen, Multi-kink solutions and soliton fission and fusion of Sharma-Tasso-Olver equation, Phys. Lett. A 374 (2010) 2340–2345.
[25] H.O. Roshid, M.M. Rashidi, Multi-soliton fusion phenomenon of Burgers equation and fission, fusion phenomenon of Sharma–Tasso–Olver equation, J. Ocea. Eng. Sci. 2 (2017) 120–126.
[26] H.O. Roshid, Lump solutions to a (3+ 1)-dimensional potential-Yu–Toda–Sasa–Fukuyama (YTSF) like equation, Int. J. Appl. Comput. Math. 3 (2017) 1455–1461.
[27] J.B. Zhang, W.X. Ma, Mixed lump-kink solutions to the BKP equation, Comput. Math. Appl. 74 (2017) 591–596.
[28] H.Q. Zhao, W.X. Ma, Mixed lump–kink solutions to the KP equation, Comput. Math. Appl. 74 (2017) 1399–1405.
[29] Y. Tang, S. Tao, Q. Guan, Lump solitons and the interaction phenomena of them for two classes of nonlinear evolution equations, Comput. Math. Appl. 72 (2016) 2334–2342.
[30] X. Zhang, Y. Chen, Rogue wave and a pair of resonance stripe solitons to a reduced (3+1)-dimensional Jimbo-Miwa equation, Commun. Nonlinear Sci. Numer. Simulat. 52 (2017) 24–31.

[31] B. Ren, W.X. Ma, J. Yu, Rational solutions and their interaction solutions of the (2+1)-dimensional modified dispersive water wave equation, Comput. Math. Appl. 77 (2019) 2086–2095.
[32] A.S. Fokas, D.E. Pelinovsky, C. Sulaem, Interaction of lumps with a line soliton for the DSII equation, Physica D 152–153 (2001) 189–198.
[33] H.O. Roshid, W.X. Ma, Dynamics of mixed lump-solitary waves of an extended (2 + 1)-dimensional shallow water wave model, Phys. Lett. A 382 (2018) 3262–3268.
[34] W.X. Ma, X. Yong, H.Q. Zhang, Diversity of interaction solutions to the (2+1)-dimensional Ito equation, Comput. Math. Appl. 75 (2018) 289–295.
[35] Y. Tang, S. Tao, M. Zhou, Q. Guan, Interaction solutions between lump and other solitons of two classes of nonlinear evolution equations, Nonlinear Dynam. 89 (2017) 1–14.
[36] Z.H. Xu, H.L. Chen, Z.D. Dai, Rogue wave for the (2+1)-dimensional Kadomtsev-Petviashvili equation, Appl. Math. Lett. 37 (2014) 34–38.
[37] J.Y. Yang, W.X. Ma, Z.Y. Qin, Lump and lump-soliton solutions to the (2+1)-dimensional Ito equation, Anal. Math. Phys. 8 (2017) 427–436.
[38] M. Shahriari, J. Manafian, Analytical behaviour of lump solution and interaction phenomenon to the Kadomtsev–Petviashvili-like equation, Pramana – J. Phys. 93 (2019) 3.
[39] M.S. Khatun, M.F. Hoque, M.A. Rahman, Multisoliton solutions, completely elastic collisions and non-elastic fusion phenomena of two PDEs, Pramana – J. Phys. 88 (2017) 86.
[40] H. Gao, Dynamics of N th-order rogue waves in (2+1)-dimensional Hirota equation, Pramana – J. Phys. 88 (2017) 84.
[41] Z. Lu, E.M. Tian, R. Grimshaw, Interaction of two lump solitons described by the Kadomtsev–Petviashvili I equation, Wave Motion 40 (2004) 123–135.
[42] Z.J. Lian, S.Y. Lou, Symmetries and exact solutions of the Sharma-Tasso-Olver equation, Nonlinear Anal. 63 (2005) 1167–1177.
[43] A.M. Wazwaz, S.A.E. Tantawy, New (3+1)-dimensional equations of Burgers type and Sharma-Tasso-Olver type: multiple-soliton solutions, Nonlinear Dynam. 87 (2017) 2457–2461.